CHINESE OPTICS LETTERS

Vol. 20, No. 12 | December 2022

Frequency control of a lattice laser at 759 nm by referencing to Yb clock transition at 578 nm

Yaqin Hao (郝雅琴), Yuan Yao (姚 远)*, Haosen Shi (师浩森), Hongfu Yu (于洪浮), Yanyi Jiang (蒋燕义), and Longsheng Ma (马龙生)

State Key Laboratory of Precision Spectroscopy, East China Normal University, Shanghai 200062, China

*Corresponding author: yyao@lps.ecnu.edu.cn

Received April 5, 2022 | Accepted June 17, 2022 | Posted Online September 23, 2022

We present the frequency control of a 759 nm laser as a lattice laser for an ytterbium (Yb) optical clock. The frequency stability and accuracy are transferred from the Yb optical clock via an optical frequency comb. Although the comb is frequency-stabilized on a rubidium microwave clock, the frequency instability of the 759 nm laser is evaluated at the 10^{-15} level at 1 s averaging time. The frequency of the 759 nm laser is controlled with an uncertainty within 1 Hz by referencing to the Yb clock transition. Such a frequency-controlled 759 nm laser is suitable for Yb optical clocks as the lattice laser. The technique of laser frequency control can be applied to other lasers in optical clocks.

Keywords: optical clock; optical frequency comb; laser frequency stabilization.
DOI: 10.3788/COL202220.120201

1. Introduction

In the last decade, tremendous progress in optical atomic clocks has been made: the frequency instability and uncertainty of optical atomic clocks have reached 10^{-18} or even 10^{-19}[1–4], two orders of magnitude better than the current definition of the second. Such accurate optical clocks have important applications in searching for possible variations of fundamental constants[5], relativistic geodesy[4], test of fundamental symmetries[6], and detection of gravitational waves[7] and dark matter[8].

Compared with single ion optical clocks, optical lattice clocks based on thousands of neutral atoms have much lower quantum projection noise-limited frequency instability due to a larger atom number[1,4]. An optical lattice is employed to confine neutral atoms in the Lamb–Dick regime, which removes the first-order Doppler shift and the photon recoil shift[9], and thus it allows Doppler-free high spectral resolution. However, the strong electric field of the lattice light will induce non-ignorable Stark shifts in both the lower and upper states of the clock transition. To cancel the light shifts, the frequency of the lattice light must be stabilized at a specific wavelength, named the magic wavelength[10–14].

Reference cavities made of ultralow expansion (ULE) glass are commonly employed to stabilize the frequency of lattice lasers[11,14,15]. Since the length of reference cavities changes due to temperature fluctuation and aging, the frequency of these cavity-stabilized lattice lasers drifts typically on the order of 10–100 kHz in a day, even the temperature of the reference cavities is stabilized with a fluctuation less than 10 mK. In an alternative method, transfer cavities referenced to atomic transitions are used to stabilize the frequency of lattice lasers, and the long-term frequency fluctuations of the lattice lasers are on the order of the megahertz (MHz) level, limited by the fluctuations of cavity dispersion[16]. In the above two methods, additional optical cavities are employed. In order to reduce the Stark shift induced by lattice light to an uncertainty of 10^{-18}, the frequency of lattice lasers must be periodically calibrated with an uncertainty of 1 MHz via optical frequency combs.

Optical frequency combs are powerful tools for measuring and controlling optical frequencies[17,18], which makes them irreplaceable in applications of optical clocks, such as frequency comparison between optical atomic clocks based on different species and absolute frequency measurement relative to cesium primary standards. Using an optical frequency comb, Bothwell *et al.* stabilized the frequency of the lattice light to a clock laser[12], whose frequency is resonant on the transition of Sr atoms. Therefore, the frequency of the lattice laser is traceable to the Sr optical clock, and the laser frequency calibration is not necessary. In this method, there is no extra optical cavity. However, the optical frequency comb is required to be tightly locked on the clock laser to achieve narrow-linewidth comb lines, which is a challenge for long-time operation.

Although optical combs frequency-stabilized to microwave standards are more robust, and their continuous operation time is longer[19], the frequency noise of such combs is much higher, compared to those stabilized to a narrow-linewidth laser. To overcome this problem, Pizzocaro *et al.* employed a Ti:sapphire laser with a linewidth of 20 kHz as the lattice laser, whose

frequency is monitored for compensating the slow frequency drift via an optical frequency comb referenced on a hydrogen maser[20]. For another, with the transfer oscillator scheme and self-referenced time base, we have realized high precision frequency transfer from a narrow-linewidth laser to a free-running laser without degrading the laser coherence even by using an optical frequency comb frequency-stabilized to a rubidium (Rb) clock[21].

In this work, we apply such a technique to realize the frequency control of a lattice laser at 759 nm. The 759 nm laser is referenced to a clock laser at 578 nm of an ytterbium (Yb) optical clock via an optical frequency comb as a transfer oscillator. The optical frequency comb is frequency-stabilized to a commercial Rb clock for long-term continuous operation. Although the frequency noise of the comb tooth (10^{-11} at 1 s average time) is much worse than that of the clock laser (2×10^{-16} at 1 s average time)[22], the additional frequency noise induced by the transfer system is characterized to be 3.7×10^{-17} at 1 s average time, benefiting from the ability to be immune from comb frequency noise. The frequency instability of the lattice laser reaches 10^{-15} at 1 s averaging time, limited by the length fluctuation of the optical fiber. The laser frequency is controlled with an accuracy of 1 Hz, good enough as a lattice laser for Yb opical clocks. Such a technique supports coherence transfer as well as frequency calibration at the same time, and it can be applied to other lasers used in optical atomic clocks.

2. Experimental Setup

The experimental setup of frequency control of the lattice laser at 759 nm is shown in Fig. 1. The 759 nm laser is a Ti:sapphire continuous wave (cw) laser pumped by a laser at 532 nm (Matisse, Spectra-Physics). The output power is more than 1 W, and the linewidth is less than 1 MHz. A small part of the light beam with a power of 10 mW is sent to an optical frequency comb for frequency control via a piece of optical fiber without fiber noise cancellation.

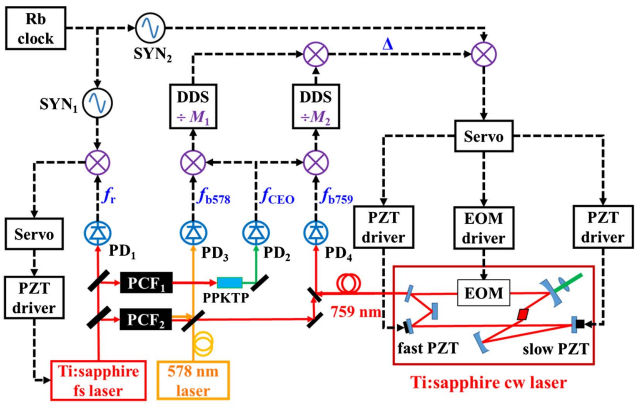

Fig. 1. Experimental set-up for frequency control of the 759 nm laser. The solid lines represent the light path, while the dashed lines represent the electrical path. Ti:sapphire fs laser, Ti:sapphire femtosecond laser; PCF, photonic crystal fiber; PPKTP, periodically poled $KTiOPO_4$; DDS, direct digital synthesizer; EOM, electro-optic modulator; PZT, piezo-transducer; Ti:sapphire cw laser, Ti:sapphire continuous wave laser; PD, photo detector; SYN, RF synthesizer.

A Ti:sapphire mode-locked femtosecond (fs) laser operates with an average output power of 1.8 W and a repetition rate (f_r) of 1 GHz. A small part of the mode-locked laser is used to generate f_r by a photo detector. In order to optimize the signal to noise ratio (SNR) of the carrier-envelope offset signal (f_{CEO}) and the beating signal between the comb teeth and the cw lasers independently, the mode-locked laser is coupled into two pieces of photonic crystal fiber (PCF). The output of PCF_1 is focused into a periodically poled $KTiOPO_4$ (PPKTP) crystal to detect f_{CEO} in the set-up of collinear $1f$–$2f$ self-referencing[23]. In order to keep the following beating signals within the bandwidth of band pass filters, both f_{CEO} and f_r are phase-locked on a commercial Rb clock (FS725).

The output of PCF_2 beats with a cavity-stabilized laser at 578 nm (ν_{578})[22] and the 759 nm laser (ν_{759}), which correspond to the clock laser and the lattice laser of the Yb optical clock, respectively. The PCFs are sealed in an aluminum tube with end facet beam expansion, enabling long-time and robust running. The average power at the output of each PCF is ~260 mW. The SNR of the beat signals is better than 30 dB with a 300 kHz resolution bandwidth (RBW). The frequencies of the beat signals between the comb and the cw lasers are

$$f_{\mathrm{b578}} = \nu_{578} - f_{\mathrm{CEO}} - N_1 f_r, \tag{1}$$

$$f_{\mathrm{b759}} = \nu_{759} - f_{\mathrm{CEO}} - N_2 f_r, \tag{2}$$

where N_1 and N_2 are integers associated with the particular comb lines. With the transfer oscillator scheme[24], the frequency noise of the comb is removed by using double balance mixers (DBMs) and direct digital synthesizers (DDSs). Specifically, we subtract the frequency noise of f_{CEO} from f_{b759} and f_{b578} by mixing them with f_{CEO}. The resulting signals are

$$f^*_{\mathrm{b578}} = \nu_{578} - N_1 f_r, \tag{3}$$

$$f^*_{\mathrm{b759}} = \nu_{759} - N_2 f_r. \tag{4}$$

These signals are then sent to two DDSs with divisors M_1 and M_2, respectively. The divisors of M_1 and M_2 are set to satisfy

$$M_1/N_1 = M_2/N_2. \tag{5}$$

The outputs of the DDSs are mixed in a DBM to subtract the frequency noise of f_r. The output of the mixer is

$$\Delta = \nu_{578}/M_1 - \nu_{759}/M_2. \tag{6}$$

By phase locking Δ to a reference signal, we can transfer the spectral purity and frequency stability of the 578 nm laser to the lattice laser at 759 nm. The actuator of the 759 nm laser for frequency control is an intra-cavity electro-optic modulator (EOM) and a fast and slow piezo-transducers (PZTs). For the

EOM, two KDP crystals at Brewster's angle are used to compensate beam displacement, and a servo bandwidth of more than 100 kHz is provided. The PZTs are employed to compensate the long-term laser frequency drift, and the servo bandwidth of the slow (fast) PZT is 1 (10) kHz.

We employ the frequency-locked laser at 759 nm as the lattice laser in an Yb optical clock. As shown in Fig. 2(a), a large part of the 759 nm laser is coupled into a piece of polarization maintenance (PM) optical fiber. The light output from the optical fiber is focused by a lens, and it is reflected by a dichroic curved mirror to build up an optical lattice with a trap depth of $U = 200E_r$ (E_r is recoil energy). The intensity of the lattice light is stabilized by adjusting the driving power of an acousto-optic modulator (AOM_1) placed before the optical fiber. Thus, the lattice trap depth is stabilized, too. The beam of the lattice light is formed vertically, but offsets from the gravity by an angle of 5°. Here, the dichroic mirror is used to reflect the 759 nm light and transmit the 578 nm light at the same time. The intensity of the 578 nm laser as the probe light is stabilized by controlling the driving power of AOM_2.

Cooling and trapping of Yb atoms are performed through a two-stage magneto-optical trap (MOT) using a strong transition of $^1S_0 \rightarrow {}^1P_1$ at 399 nm and a narrower transition of $^1S_0 \rightarrow {}^3P_1$ at 556 nm. After the atoms are loaded into the optical lattice[25], a linearly polarized 556 nm pulse and a bias magnetic field are applied for spin polarization. Then, the clock transition of $^1S_0 \rightarrow {}^3P_0$ is probed with the 578 nm laser. The excitation rate is measured by applying three pulses at 399 nm and a pulse at 1389 nm[25]. The 399 nm beam for detection strongly saturates the $^1S_0 \rightarrow {}^1P_1$ transition with a power of 1 mW. The first 399 nm pulse measures the population of the $^1S_0$ state. The second 399 nm pulse measures the population of the $^3P_0$ state after repumping the excited atom population over the short-lived $^3D_1$ level back to the $^1S_0$ with a 1389 nm pulse. The 10 mW beam at 1389 nm is resonant with the transition of $^3P_0 - {}^3D_1$, and the repumping efficiency is 90% after 5 ms. The third 399 nm pulse then reveals the background signal from scattered light and excited hot gas atoms. The fluorescence from the three 399 nm pulses is collected with a photomultiplier tube (PMT), and, for each pulse, the PMT signal is digitally integrated for 5 ms. The signals are used to digitally calculate the normalized excitation fraction and the total number of atoms. With an atomic probe time of 200 ms, a Rabi spectrum with 4.3 Hz linewidth is obtained [Fig. 2(b)].

Based on the above spectra with a linewidth of ~4 Hz, we tune the frequency of the 578 nm laser to be resonant with the atomic clock transition. We use the measured excitation rate as a frequency discriminator to stabilize the 578 nm laser to the atomic clock transition by feeding back to the driving frequency of AOM_3. There are four interrogations in each feedback cycle of 2.2 s. Two of them are used to interrogate the $^1S_0$ ($m_F = +1/2$) $\rightarrow {}^3P_0$ ($m_F = +1/2$) transition, and the other two are used to interrogate the $^1S_0$ ($m_F = -1/2$) $\rightarrow {}^3P_0$ ($m_F = -1/2$) transition with the frequency of the 578 nm laser set at the shoulders of the transitions. The cavity-stabilized 578 nm laser is further locked to the average frequency of the two $m_F = \pm 1/2$ components in order to remove the first-order Zeeman shift and the vector lattice shift. When the frequency of the 578 nm laser is locked on the clock transition, the frequency of the lattice laser is

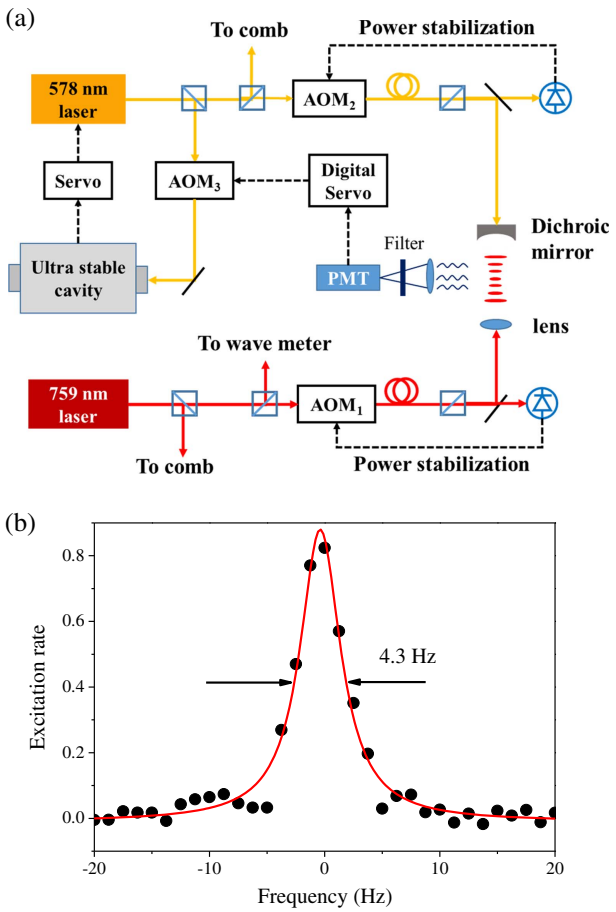

Fig. 2. (a) Simplified experimental set-up for optical clock operation. (b) Rabi spectrum with a probe time of 200 ms.

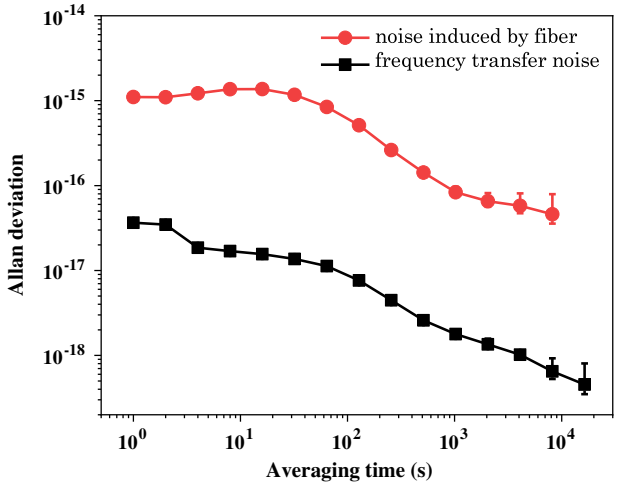

Fig. 3. Frequency noise induced by a 10-m-long fiber (red dots) and in-loop frequency noise during frequency transfer (black squares).

known as

$$\nu_{759} = M_2 \times (\nu_{\text{clock}}/M_1 - \Delta), \tag{7}$$

where ν_{clock} is the center frequency of the clock transition.

3. Results

To evaluate the frequency instability induced by the transfer process, the frequency of Δ is recorded on a frequency counter with a gate time of 1 s. The time base of the synthesizers and the counter is the Rb clock. The additional frequency noise onto the 759 nm laser induced in the laser frequency control is 3.7×10^{-17} at 1 s average time, as shown with black squares in Fig. 3. The frequency instability of the 578 nm laser is 2×10^{-16} at 1 s average time[22], and it is $5.5 \times 10^{-16}/\sqrt{\tau}$ after further stabilization to the Yb clock transition[26]. The short-term instability of the clock is limited by the gain of feedback and the Dick effect[27,28]. Therefore, the frequency instability of the 759 nm laser is evaluated to be on the order of 10^{-15} at 1 s averaging time, which is mainly limited by the length fluctuation of the optical fiber (as shown with red dots in Fig. 3).

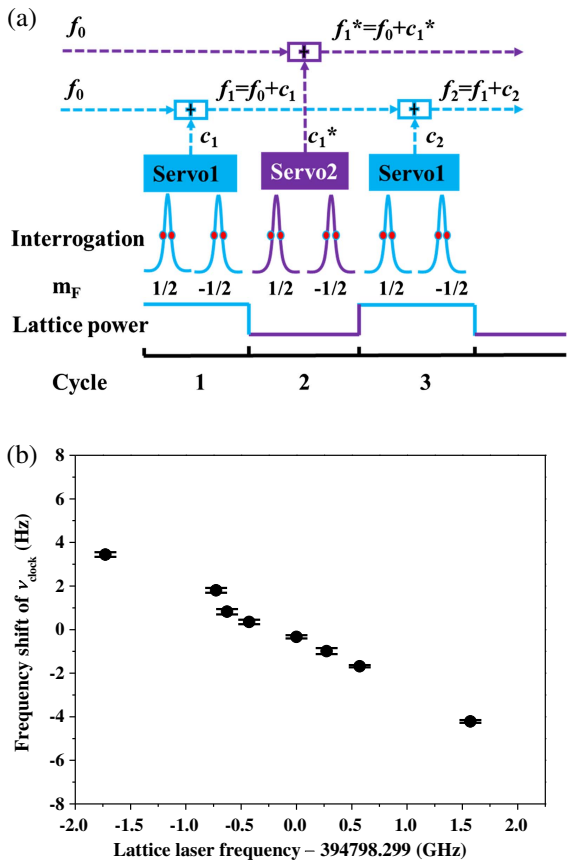

Fig. 4. (a) Timing sequence of self-comparison. Blue and purple lines indicate two independent stabilizations. (b) Scalar lattice shift at $U = 200E_r$ measured by interleaving between a trap depth of $158(4)E_r$ and $226(4)E_r$ at different lattice frequencies.

The frequency accuracy of the lattice laser is also evaluated. According to Eq. (7), the frequency of the 759 nm laser is dependent on the divisors of the DDSs, Δ, and ν_{clock}. It has been demonstrated in the previous report[21] that the inaccuracy induced by the DDSs is less than 1 μHz. In our system, the frequency of Δ is 98 MHz, and M_2 is about four. Since Δ is referenced to the Rb clock with a frequency uncertainty of 5×10^{-10}, the frequency uncertainty of $M_2 \times \Delta$ is 0.2 Hz.

Since ν_{759} is referenced to ν_{clock} according to Eq. (7), we experimentally study the frequency shift of ν_{clock} when the frequency of the lattice laser is set at different frequencies. We interleave two clock cycles operating at different lattice intensities[29]. As shown in Fig. 4(a), two independent servos are employed to separately calculate the correction signals c_i and c_i^* for feeding back to the driving signals of AOM_3 (f_i and f_i^*). We use $f_i - f_i^*$ to represent the frequency difference of the clock transitions in a high and a low trap depth of $U_H = 226(4)E_r$ and $U_L = 158(4)E_r$. The resulting shift at $U = 200E_r$ is calculated since the frequency shift is approximately linear to trap depth when $U < 300E_r$[20]. The trap depths are determined by the sideband spectroscopy of clock transition. The lattice laser frequency is measured by the comb referenced on the Rb clock. The frequency shift of the clock transition as a function of the lattice frequency is shown in Fig. 4(b). At $U = 200E_r$, the frequency shift of ν_{clock} is less than ±5 Hz when the lattice frequency is detuned from the working point within ±1.5 GHz. Since the frequency of the lattice laser is monitored on a wavemeter with an uncertainty of 60 MHz, the frequency shift of ν_{clock} can be kept within 0.2 Hz. As $M_2/M_1 \approx 0.76$, the inaccuracy induced by ν_{clock} is 0.15 Hz. In a normal case, the frequency uncertainty of ν_{clock} contributed by other effects is less than 1 Hz[4,15,20]. Therefore, the frequency uncertainty of ν_{759} is less than 1 Hz, considering the uncertainty of ν_{clock} and Δ.

4. Conclusion

We report a frequency-controlled lattice laser at 759 nm by referencing to a clock laser at 578 nm via an optical frequency comb stabilized to a Rb clock. The frequency instability of the lattice laser is on the order of 10^{-15} at 1 s averaging time, and the frequency uncertainty is less than 1 Hz. Using this method, it does not need an extra cavity for frequency stabilization or laser frequency calibration. This method can be applied for frequency stabilization of other lasers in optical clocks.

Acknowledgement

This work was supported by the National Natural Science Foundation of China (No. 11927810).

References

1. E. Oelker, R. B. Huston, C. J. Kennedy, L. Sonderhouse, T. Bothwell, A. Goban, D. Kedar, C. Sanner, J. M. Robinson, G. E. Marti, D. G. Matei, T. Legero, M. Giunta, R. Holzwarth, F. Riehle, U. Sterr, and J. Ye,

"Demonstration of 4.8×10^{-17} stability at 1 s for two independent optical clocks," Nat. Photon. **13**, 714 (2019).
2. N. Huntemann, C. Sanner, B. Lipphardt, C. Tamm, and E. Peik, "Single-ion atomic clock with 3×10^{-18} systematic uncertainty," Phys. Rev. Lett. **116**, 063001 (2016).
3. S. M. Brewer, J. S. Chen, A. M. Hankin, E. R. Clements, C. W. Chou, D. J. Wineland, D. B. Hume, and D. R. Leibrandt, "$^{27}Al^+$ quantum-logic clock with a systematic uncertainty below 10^{-18}," Phys. Rev. Lett. **123**, 033201 (2019).
4. W. F. McGrew, X. Zhang, R. J. Fasano, S. A. Schäffer, K. Beloy, D. Nicolodi, R. C. Brown, N. Hinkley, G. Milani, M. Schioppo, T. H. Yoon, and A. D. Ludlow, "Atomic clock performance enabling geodesy below the centimetre level," Nature **564**, 87 (2018).
5. M. S. Safronova, D. Budker, D. DeMille, D. F. J. Kimball, A. Derevianko, and C. W. Clark, "Search for new physics with atoms and molecules," Rev. Mod. Phys. **90**, 025008 (2018).
6. C. Sanner, N. Huntemann, R. Lange, C. Tamm, E. Peik, M. S. Safronova, and S. G. Porsev, "Optical clock comparison for Lorentz symmetry testing," Nature **567**, 204 (2019).
7. S. Kolkowitz, I. Pikovski, N. Langellier, M. D. Lukin, R. L. Walsworth, and J. Ye, "Gravitational wave detection with optical lattice atomic clocks," Phys. Rev. D **94**, 124043 (2016).
8. B. M. Roberts, G. Blewitt, C. Dailey, M. Murphy, M. Pospelov, A. Rollings, J. Sherman, W. Williams, and A. Derevianko, "Search for domain wall dark matter with atomic clocks on board global positioning system satellites," Nat. Commun. **8**, 1195 (2017).
9. C. I. Westbrook, R. N. Watts, C. E. Tanner, S. L. Rolston, W. D. Phillips, P. D. Lett, and P. L. Gould, "Localization of atoms in a three-dimensional standing wave," Phys. Rev. Lett. **65**, 33 (1990).
10. T. Ido and H. Katori, "Recoil-free spectroscopy of neutral Sr atoms in the Lamb-Dicke regime," Phys. Rev. Lett. **91**, 053001 (2003).
11. I. Ushijima, M. Takamoto, and H. Katori, "Operational magic intensity for Sr optical latice clock," Phys. Rev. Lett. **121**, 263202 (2018).
12. T. Bothwell, D. Kedar, E. Oelker, J. M. Robinson, S. L. Bromley, W. L. Tew, J. Ye, and C. J. Kennedy, "SrI optical lattice clock with uncertainty of 2×10^{-18}," Metrologia **56**, 065004 (2019).
13. M. J. Zhang, H. Liu, X. Zhang, K. L. Jiang, Z. X. Xiong, B. L. Lu, and L. X. He, "Hertz-level clock spectroscopy of ^{171}Yb atoms in a one-dimensional optical lattice," Chin. Phys. Lett. **33**, 070601 (2016).
14. R. C. Brown, N. B. Phillips, K. Beloy, W. F. McGrew, M. Schioppo, R. J. Fasano, G. Milani, X. Zhang, N. Hinkley, H. Leopardi, T. H. Yoon, D. Nicolodi, T. M. Fortier, and A. D. Ludlow, "Hyperpolarizability and operational magic wavelength in an optical lattice clock," Phys. Rev. Lett. **119**, 253001 (2017).
15. Q. Gao, M. Zhou, C. Y. Han, S. Y. Li, S. Zhang, Y. Yao, B. Li, H. Qiao, D. Ai, G. Lou, M. Y. Zhang, Y. Y. Jiang, Z. Y. Bi, L. S. Ma, and X. Y. Xu, "Systematic evaluation of a ^{171}Yb optical clock by synchronous comparison between two lattice systems," Sci. Rep. **8**, 8022 (2018).
16. P. G. Westergaard, J. Lodewyck, L. Lorini, A. Lecallier, E. A. Burt, M. Zawada, J. Millo, and P. Lemonde, "Lattice-induced frequency shifts in Sr optical lattice clocks at the 10^{-17} level," Phys. Rev. Lett. **106**, 210801 (2011).
17. J. L. Hall, "Nobel lecture: defining and measuring optical frequencies," Rev. Mod. Phys. **78**, 1279 (2006).
18. T. W. Hänsch, "Nobel lecture: passion for precision," Rev. Mod. Phys. **78**, 1297 (2006).
19. G. Yang, H. S. Shi, Y. Yao, H. F. Yu, Y. Y. Jiang, A. Bartels, and L. S. Ma, "Long-term frequency-stabilized optical frequency comb based on a turnkey Ti:sapphire mode-locked laser," Chin. Opt. Lett. **19**, 121405 (2021).
20. M. Pizzocaro, P. Thoumany, B. Rauf, F. Bregolin, G. Milani, C. Clivati, G. A. Costanzo, F. Levi, and D. Calonico, "Absolute frequency measurement of the $^1S_0$–$^3P_0$ transition of ^{171}Yb," Metrologia **54**, 102 (2017).
21. Y. Yao, B. Li, G. Yang, X. T. Chen, Y. Q. Hao, H. F. Yu, Y. Y. Jiang, and L. S. Ma, "Optical frequency synthesizer referenced to an ytterbium optical clock," Photon. Res. **9**, 98 (2021).
22. L. Jin, Y. Y. Jiang, Y. Yao, H. F. Yu, Z. Y. Bi, and L. S. Ma, "Laser frequency instability of 2×10^{-16} by stabilizing to 30-cm-long Fabry-Perot cavities at 578 nm," Opt. Express **26**, 18699 (2018).
23. Y. Y. Jiang, Z. Y. Bi, R. Lennart, and L. S. Ma, "A collinear self-referencing setup for control of the carrier-envelope offset frequency in Ti:sapphire femtosecond laser frequency combs," Metrologia **42**, 304 (2005).
24. H. R. Telle, B. Lipphardt, and J. Stenger, "Kerr-lens, mode-locked lasers as transfer oscillators for optical frequency measurements," Appl. Phys. B **74**, 1 (2002).
25. W. Nagourney, J. Sandberg, and H. Dehmelt, "Shelved optical electron amplifier: observation of quantum jumps," Phys. Rev. Lett. **56**, 2797 (1986).
26. Y. X. Sun, Y. Yao, Y. Q. Hao, H. F. Yu, Y. Y. Jiang, and L. S. Ma, "Laser stabilizing to ytterbium clock transition with Rabi and Ramsey spectroscopy," Chin. Opt. Lett. **18**, 070201 (2020).
27. Y. Y. Jiang, A. D. Ludlow, N. D. Lemke, R. W. Fox, J. A. Sherman, L. S. Ma, and C. W. Oates, "Making optical atomic clocks more stable with 10^{-16}-level laser stabilization," Nat. Photon. **5**, 158 (2011).
28. T. L. Nicholson, M. J. Martin, J. R. Williams, B. J. Bloom, M. Bishof, M. D. Swallows, S. L. Campbell, and J. Ye, "Comparison of two independent Sr optical clocks with 1×10^{-17} stability at 103 s," Phys. Rev. Lett. **109**, 230801 (2012).
29. Q. Wang, Y. G. Lin, F. Meng, Y. Li, B. K. Lin, E. J. Zang, T. C. Li, and Z. J. Fang, "Magic wavelength measurement of the ^{87}Sr optical lattice clock at NIM," Chin. Phys. Lett. **33**, 103201 (2016).